

TIME AND STRESS EFFECTS ON THE SURFACE MORPHOLOGY OF PMMA UNDER FATIGUE

GUILLERMO C. PULOS
*Instituto de Investigaciones en Materiales, UNAM
México, D.F. 04510*

ABSTRACT

The effects of stress level and frequency on fatigue cracks have been studied with a special loading device that allows precise load and displacements prescription and uses optical microscopy to determine the crack length with a resolution of 1 to 2 microns. Measurements at three different stress intensity factors levels produce features on the fracture surface that range from coherent (or through-the-specimen-thickness) markings with length scales smaller than the length of the craze, to incoherent features, the scale of which are two to four times larger than the craze; crack growth occurs with decelerating/accelerating stages while it forms the incoherent surface markings. Coherent markings correspond to discontinuous or retarded crack growth. The changes in surface morphology are the result of increased stress and/or reduced process time defined as the time it takes a fibril to travel from the tip to the trailing end of the craze. The crack/craze front slows down as it travels through the incoherent (and sometimes rougher) features of the fracture surface. Evidence begins to emerge that the time history of loading has a first order effect on surface features and mode of failure at the crack tip through the time rate of cracktip deformations.

KEYWORDS

Deceleration/acceleration stages, incoherent surface morphology, thermoplastics, crazing, PMMA, fatigue.

INTRODUCTION

Propagation of fatigue cracks in thermoplastics has been characterized "bimodally" as Normal Crack Growth (NCG) or as Retarded (or Discontinuous) Crack Growth (RCG). In NCG the crack is believed to grow by the same amount in each cycle and without a change in the craze length; thus, the crack and craze tips propagate with the same speed and in phase with each other. By contrast, RCG is identified as the process during which the crack is considered to remain stationary for a number of cycles (e.g. ~ a few hundred cycles) while the craze increases in size and then, during one particular cycle, the crack jumps through about 1/2 to 2/3 of the length of the craze: in this case, crack and craze growth are completely out of phase and the average growth rate is the jump distance divided by the number of cycles between jumps. RCG was first reported by Elinck et al. (1971) who noticed that markings on the fracture surface matched the growth rate for jumps occurring about every 370 cycles. Using optical

interferometry, real-time measurements of RCG have been made by observing the craze at the tip of a crack, as documented by Döll and Könczöll in their excellent review article (1990); both NCG and RCG are described by Hertzberg and Manson (1980).

The difference between NCG and RCG is determined by two different processes. One is the rate of fibrillation at the tip of the craze where the bulk material transforms into craze material; the other is the rate of failure of the fibrils along the base or trailing end of the craze (at the crack tip proper). During RCG, both processes are out of phase with respect to each other; the crack remains stationary for a number of cycles while fibrillation enlarges the craze; then, during one particular cycle, the crack breaks through the craze or through a part of it. Implicit here is the idea that the length scales involved (jump distances) are equal to or smaller than the length of the craze. However, an alternative mode of RCG is possible in which the crack does not stop but propagates in a non-steady fashion with decelerating and accelerating stages. When growth occurs in this fashion, intermediate to the normal and retarded modes, the markings generated by the craze and left on the fracture surface can have dimensions larger than the craze itself as the craze enlarges and contracts while on a moving reference frame (crack tip).

To determine such a nonsteady crack growth process, as well as quantify the (fluctuating) periodicity of the accelerating/decelerating stages requires enough measurements of the crack length in units significantly smaller than the size of the craze. Thus, real-time optical measurements are used here to determine the crack length with a resolution of about 2 microns (1/20 of the craze length) once (or many times) during each cycle of fatigue experiments as the crack grows over distances of several millimeters.

EXPERIMENTAL SET-UP

Experiments on the history of crack tip motion in compact tension PMMA specimens¹ were carried out using a high-precision miniature loading device; the set-up, including the optical arrangement, illumination and data collection, has been discussed by Pulos and Knauss (1996). The measurements of the crack length were made on the surface of the specimen and, as it will be shown later, correlate well with fracture advance inside the specimen as shown on the surface morphology. Optical measurements to detect the length and shape of the craze that precedes the crack through the specimen can only be made in NCG or during RCG when the markings are coherent or through-the-thickness; thus, when the crack/craze system leaves incoherent surfaces on the fracture surface, the length of the craze is estimated via a Barenblatt/Dugdale analysis.

CRACK LENGTH DEVIATION

It is customary in crack propagation studies under fatigue loading to record the crack propagation rate as a function of a stress intensity variation (ΔK) under the assumption that the crack propagates with a constant rate and assigns an average propagation rate to such a measurement. Here interest centers on the *variation* in crack propagation from such an average in order to assess the (possible) lack of steadiness in the propagation behavior. To this end define the "crack length deviation" ("crack deviation" for short) as the difference between the average location of the crack tip² and the measured value at any instant of time. Thus if the crack accelerates and decelerates *as it progresses* the deviation should be a cyclical kind of record with time-averaged zero value.

¹The specimens are 32 mm wide, 40 mm long and 3 mm thick. The material used was commercial PMMA from Rohm and Haas (Plexiglas G) and medium molecular weight PMMA from Aldrich.

²expressed by a least squares fit of a straight line to the crack propagation data

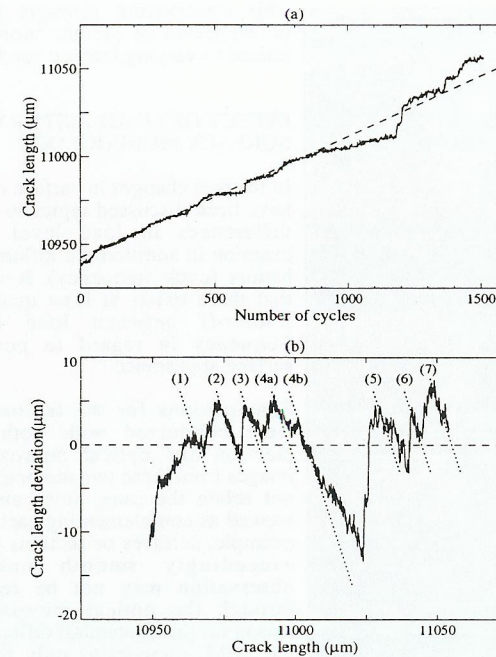


Fig. 1 Crack length (a) and crack length deviation (b) records of an experiment where the crack jumped by 18 μm (K_I max. 0.46 $\text{MPa m}^{1/2}$).

not very meaningful because the resolution capability of the measurement method is only a micron. Thus when very small deviations occur, one should conclude that the crack propagates -within the present resolution capability- at a very uniform rate, a situation that corresponds to the classical or "normal" crack propagation behavior (equal advances during each cycle).

This situation arises, for example, in part of Fig. 2 for the segment of growth from 14300 and 15000 μm ($K_{\text{max}} = 0.8 \text{ MPa m}^{1/2}$, $K_{\text{min}} = 0.08 \text{ MPa m}^{1/2}$, $\nu = 0.5 \text{ Hz}$). In contrast to the lower stress intensities underlying Fig. 1 the now higher frequency and higher K-values produce a different cyclic response.

Upon further increasing the frequency and the stress intensity a very unsteady crack propagation history results. This is also illustrated in Fig. 2 for the segments of crack length between (a) 13000 to 14100 μm . ($K_{\text{max}} = 0.95 \text{ MPa m}^{1/2}$, $K_{\text{min}} = 0.1 \text{ MPa m}^{1/2}$, $\nu = 2 \text{ Hz}$) and between (b) 15300 and 16000 μm ($K_{\text{max}} = 1.0 \text{ MPa m}^{1/2}$, $K_{\text{min}} = 0.1 \text{ MPa m}^{1/2}$, $\nu = 0.5 \text{ Hz}$). The formerly (optically) smooth appearing fracture surface has now become inhomogeneous with relatively large attendant crack deviations. The length scales over which these deviations extend are larger than the typical craze lengths by factors of two to five. Another feature worth stressing is that the optical appearances of the regions (a) and (b) are nearly the same, but that the loading conditions are different: Part (a) results from a stress intensity level of $K_{\text{max}} = 0.95 \text{ MPa m}^{1/2}$ while that of (b) is induced under a level of $K_{\text{max}} = 1.0 \text{ MPa m}^{1/2}$; however, the frequencies are, respectively, 2 Hz and 0.5 Hz.

Nonsteady crack propagation is illustrated in Fig. 1, where the first plot renders the crack tip position as a function of the cycle number ($K_{\text{max}} = 0.46 \text{ MPa m}^{1/2}$, $K_{\text{min}} = 0.1 \text{ MPa m}^{1/2}$, $\nu = 0.1 \text{ Hz}$; one point per cycle). The second plot illustrates the "crack deviation" which has several distinguishing features about it (crack tip proper = trailing end of craze). Since it relates the difference of the actual from the *average* position as a function of the average crack tip position a negative unit slope is synonymous with a stationary crack tip (the crack tip may still grow). Several dotted lines in that figure illustrate conditions close to temporary crack tip arrest, and it will be appreciated that excepting one or two cases the crack does not rest between spurts. During all spurts the crack advances only a fraction of the craze length; the fraction is not necessarily constant, though most of them are on the order of 12 to 25%. Similar growth behavior in PE was reported by Lu *et al.* (1991).

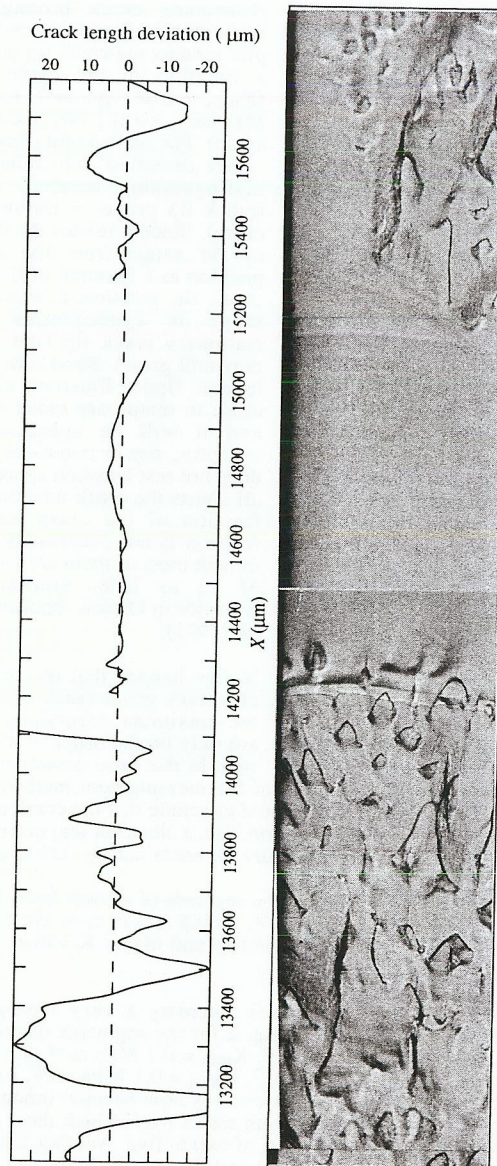


Fig. 2 Crack length deviation and fracture surface morphology at high (0.95, 1.0 Mpa $m^{1/2}$) and lower (0.8 Mpa $m^{1/2}$) K_I .

This observation prompts the further investigation of surface morphology as related to varying loading conditions

EFFECT OF LOAD HISTORY ON SURFACE MORPHOLOGY

In the past changes in surface morphology have been discussed typically in terms of differences in load level. Here we examine in addition the influence of time history (cycle frequency). It will be seen that there exists at least qualitatively a trade-off between load level and frequency in regard to post fracture surface appearance.

Examinations for the fracture surfaces were conducted with both scanning electron and optical microscopy. The images from these two methods clearly do not relate the same story and must be viewed as complementing each other. For example, surfaces or sections that appear exceedingly smooth under SEM observation may not be rendered so through the optical microscope. The reason for this (potential) difference is that the SEM interrogates only the extreme surface, which may indeed be very flat or smooth, corresponding to the (fractured) midplane of the craze. The optical microscope, however, interrogates the depth of the (fractured) craze throughout the residual craze layer thickness. Thus, if one were to conclude from the SEM observation that a featureless surface implies a uniform craze thickness, this might be quite an incorrect conclusion. Instead, significant variations in features under the optical microscope indicate a locally very varied load history during the crack propagation process.

It is useful to distinguish for discussion purposes "coherent" and "incoherent" crack propagation: The former implies that crack growth occurs along the whole crack front (smooth plan form) in the same plane with a featureless crack surface in both SEM and optical microscopy. Incoherent crack propagation is characterized by the fact that a smooth crack front no longer exists and the advance occurs with features that deviate from the common or average crack plane, associated with optical features that

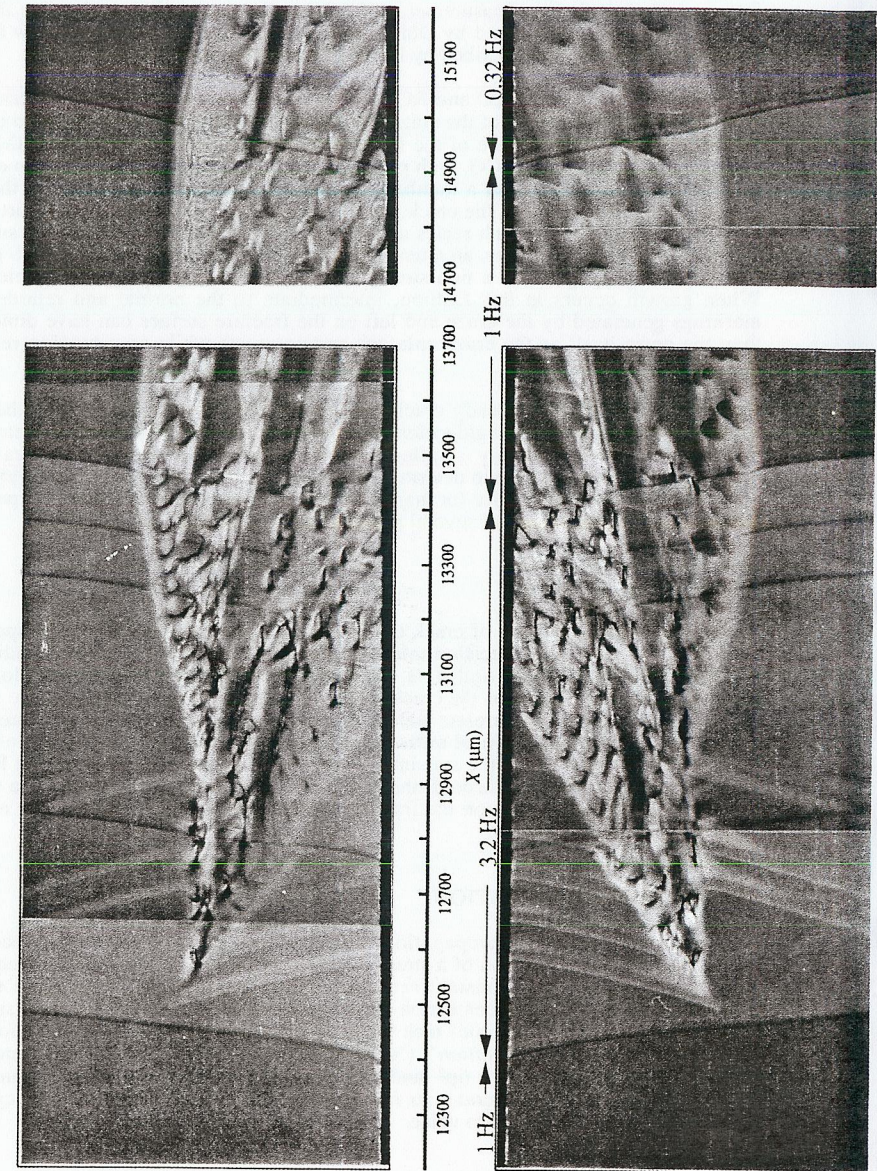


Fig. 3 Fracture surface morphology at a constant stress intensity factor (0.61 Mpa $m^{1/2}$) and test frequencies of 1 Hz, 3.2 Hz, 1 Hz and 0.32 Hz.

indicate clear variations in the craze thickness. Incoherent crack propagation can occur with large sections of the surface appearing smooth and flat in SEM examinations.

Coherent Crack Growth (Normal And Retarded)

Examples of coherent crack growth have been discussed in relation to RCG, NCG and the section on crack length deviation; this phenomenon can occur in a retardation manner at low stress intensity (c.f. Fig. 1; $K_{max} = 0.46 \text{ Mpa m}^{1/2}$, $K_{min} = 0.1 \text{ Mpa m}^{1/2}$, $\nu = 0.1 \text{ Hz}$) or as NCG (c.f. Fig. 2 from 14300 and 15000 μm ; $K_{max} = 0.8 \text{ Mpa m}^{1/2}$, $K_{min} = 0.08 \text{ Mpa m}^{1/2}$, $\nu = 0.5 \text{ Hz}$). However, under the similar stress intensity magnitudes but with a different frequency, the latter NCG turns into RCG once the frequency is reduced from 0.5 Hz to 0.32 or lower; in this case, it is possible to determine the stresses acting on the craze at the tip of a crack (see Knauss, 1996). The surface morphology of both RCG and NCG has been documented by Döll (1989).

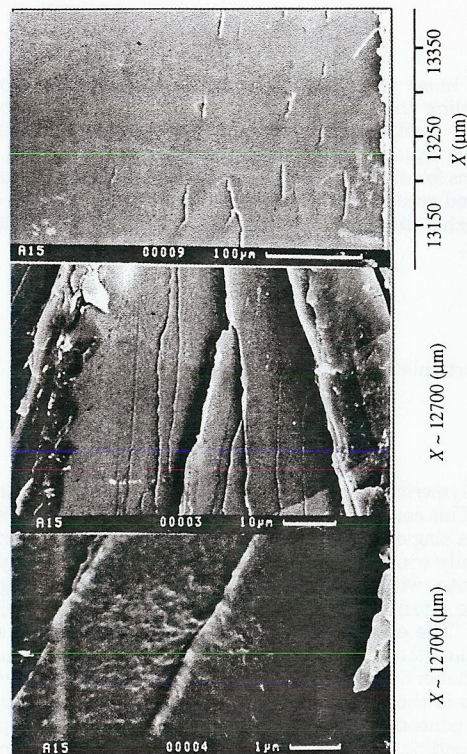


Fig. 4 SEM photographs of wedge-shaped regions.

crack propagation direction until the frequency is reduced again to 1 Hz. Under this frequency the widths of these regions then remain constant, but decrease steadily as soon as the frequency is reduced further to 0.32 Hz, disappearing, by eventually ending up in points again (see Fig. 5;

Incoherent Crack Growth; Effect of Changing the Frequency.

In the following sections reference is made to the surface appearance in three figures. in a presentation sequence different from the recording sequence: Crack propagation starts at the bottom in Fig. 3, the continuation from the top of which is documented in Fig. 5; Fig. 4 represents an SEM examination of a portion of Fig. 3. These figures result from the following load histories: $K_{max} = 0.6 \text{ Mpa m}^{1/2}$, $R = 0.1$ and, for successive crack lengths " l " as indicated with the frequencies

to $l = 12450 \mu\text{m}$	$\nu = 1 \text{ Hz}$
$12450 \mu\text{m} < l < 13500 \mu\text{m}$	$\nu = 3.2 \text{ Hz}$
$13500 \mu\text{m} < l < 14900 \mu\text{m}$	$\nu = 1 \text{ Hz}$
$14900 \mu\text{m} < l < 16400 \mu\text{m}$	$\nu = 0.32 \text{ Hz}$
from $16400 \mu\text{m}$ on	$\nu = 0.1 \text{ Hz}$.

The distinguishing features of this sequence is the successive development and then disappearance of regions of incoherent propagation. These regions occur multiply across the width of the specimen (only one region from near one side of the specimen shown in Figs. 3 -5). Initially, under 1 Hz loading one observes NCG. Soon after increasing the frequency to 3.2 Hz incoherent regions develop at isolated points and spread laterally to the

the same phenomenon occurs at the other sites across the thickness of the specimen). For reference or scaling purposes the reader is reminded that the craze length is on the order of 30 to 50 μm .

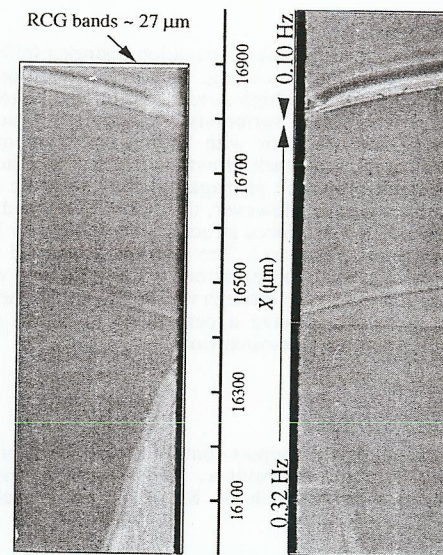


Fig. 5 Fracture surface morphology at a constant stress intensity factor ($0.61 \text{ Mpa m}^{1/2}$) and test frequencies of 0.32 Hz and 0.10 Hz.

It is truly surprising that coherent and incoherent regions can exist literally side-by-side and increase or decrease systematically through a mere change of frequency. There are apparently three-dimensional effects at work that have to do with the size and shape of the craze zone as occasioned by differences in the (nonlinearly) viscoelastic response of the craze material.

SEM examination of the incoherently produced fracture surface at about 13200 μm , shown in Fig. 4, yields an almost perfectly flat surface (at this particular magnification), except for isolated "cuts" along which the fracture propagated at different elevations through the craze. Further deductions can be made from color photographs regarding as to where the crack moves through the middle of the craze, and where closer to one side or the other. The main observation here is that the optical micrographs evidence a rich variation of the craze depth while most of the fracture surface is flat and rather free of elevation changes.

Return to Coherent Growth

Once the incoherent growth had disappeared (and the frequency was lowered) the crack propagation reverted back to discontinuous or retarded growth with surface features that are on the order of or larger than the craze length. However, this change-over did not occur instantaneously but only after a few craze length of growth in a coherent fashion.

Incoherent crack growth is associated with reduced crack propagation rates when compared with coherent growth. Figure 6 illustrates an interferometric rendition of the craze/crack front (propagation towards top of figure) with a band of incoherent growth as indicated. It is clear that in the later region the crack front lags behind that for the coherent growth. This observation applied to all situations allowing this comparison, though the

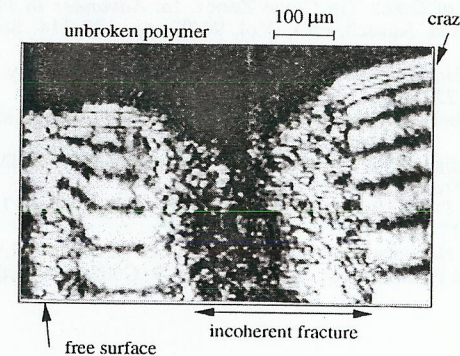


Fig. 6 Interferometric fringes of the craze and crack opening displacement showing the slow down of the craze/crack front through an incoherent feature.

numerical differences in velocity might be small (~ 20%).

CONCLUSION

Detailed time-resolved studies show that a variety of crack propagation histories follow from varying both the magnitude and the frequency of cyclic loading. Coherent crack propagation results at low stress levels and low cycling rates, while high stress intensities tend to lead to incoherent crack growth associated with large unsteady variations in crack propagation rates. Coherent crack growth can be associated with NCG or with RCG, depending on stress intensity range and frequency. RCG or discontinuous crack growth has to be understood as a more or less continuous and cyclical variation in crack propagation rate, with the cyclical advances being always smaller than the craze length. However, the optically tracked surface features such as banding (striations) or incoherently produced structures are invariably larger in size than the length of the craze zone (two to four times). The optically observed features indicate a much more turbulent character than SEM observations which reveal a very flat surface with isolated discontinuities in crack propagation through the craze. In fact, the growth and disappearance of incoherent fracture surfaces have a certain resemblance to fluid turbulence behavior as opposed to coherent growth like laminar flow.

ACKNOWLEDGMENTS

The author wishes to acknowledge various sources of support contributing to this work: ONR through grant # N00014-91-J-1427 with Dr. Peter Schmidt as the technical monitor; E.I. DuPont de Nemours Company through initial contact with Dr. Manuel Panar as well as the Newport Corporation.

REFERENCES

- Döll, W. (1989). Fractography and Failure Mechanisms of Amorphous Thermoplastics. In: *Fractography and Failure Mechanisms of Polymers and Composites* (A.C. Roulin-Moloney, ed.), pp. 387-436. Elsevier Science Publishers LTD, New York.
- Döll, W. and L. Könczöl (1990). Micromechanics of Fracture under Static and Fatigue Loading: Optical Interferometry of Crack Tip Craze Zones. In: *Advances in Polymer Science: Crazeing in Polymers* (H.H. Kausch, ed.), Vol. 91/92, pp. 137-214. Springer-Verlag, Berlin.
- Elinck, J. P., J. C. Bauwens, and G. Homes (1971). Fatigue Crack Growth in Poly (Vinyl Chloride). *Int. J. Fract. Mech.*, **7**, 277-287.
- Hertzberg, R. W. and J. A. Manson (1980). *Fatigue of Engineering Plastics*. Academic Press, New York.
- Knauss, W. G. (1996). Cohesive force distribution of crack tip crazes in fatigue of PMMA. In: *9th International Conference on Fracture*, Sidney.
- Lu, X., R. Qian, and N. Brown (1991). Discontinuous Crack Growth in Polyethylene Under a Constant Load. *J. Mat. Sci.*, **26**, 917-924.
- Pulos, G. C. and W. G. Knauss (1996). Nonsteady Crack and Craze Behavior in PMMA under Cyclical Loading: I. Experimental Preliminaries. Report SM 96-9, California Institute of Technology, Pasadena.